MATHEMATICAL MODELS OF EYE MOVEMENTS

OZGUR AKMAN, D. S. BROOMHEAD, AND R. A. CLEMENT

Introduction

If our efforts to write something of interest have been successful, a good deal of your conscious mind will—for the next half hour or so—be occupied in the act of reading. Less obviously, however, we shall also be engaging many of your unconscious brain functions. For example, as you read it is unlikely that you are aware of what your eyes are doing. In fact, a set of neural control mechanisms—mechanisms which evolved at an early stage in the development of species such as *homo sapiens*—are jerking your eyes in patterns which enable you to image the words you are reading on a small specific part of your retina. Other mechanisms maintain the position of the image by compensating for your head movements as you adjust your seating position. A fly attracts your attention (oh dear, lost you already!) as it flies noisily across the room; you look up to follow its trajectory. Again you attempt, unconsciously, to keep the image of the fly on the same small, specific part of your retina; another neural control mechanism becomes active as you do this.

The part of the retina in question is called the *fovea* (or, sometimes, the "yellow spot"); it is the part capable of high-resolution, colour imaging. Thus, when we look *at* something—as opposed to becoming aware of it in our peripheral vision—we usually arrange for its image to land on the fovea. How do we do this? The study of this issue has a long history, which has generally involved some rather ingenious science since it is difficult to observe directly the behaviour of the human brain. One important approach has concentrated on trying to understand eye movement control systems by trying to understand what can go wrong with them. This is the approach that we shall adopt here.

Congenital Nystagmus

Our work is with vision scientists [1] who are interested in a condition known as *congenital nystagmus*, an involuntary oscillation of the eyes which develops at, or shortly after, birth. About 1 in 4000 people suffer from this condition which can cause loss of visual acuity. Generally, both eyes oscillate in phase in the same plane (usually horizontally). Sometimes the amplitude of the oscillation depends on gaze direction; in this case it is not uncommon for the subject to develop an unconscious head tilt which improves vision. In figure 1 we show a plot of the eye movements of a patient with congenital nystagmus. This distinctive waveform is often referred to as "jerk nystagmus". The eye accelerates away from the desired eye position which would place the image of the target on the fovea (in the case of figure 1 this corresponds roughly to the horizontal axis) and is then jerked back to something like the correct
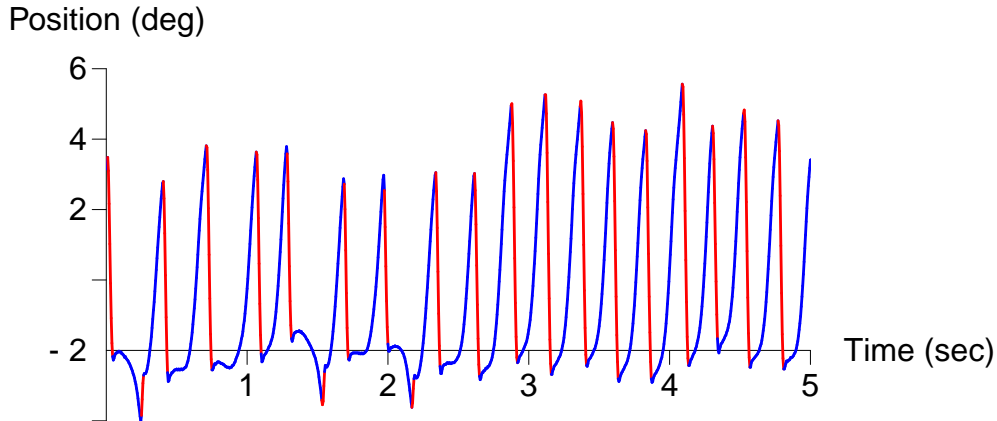
FIGURE 1. A plot of nystagmus eye movements. The subject's head
was held in place and she was asked to look directly ahead at a small,
stationary target projected onto a screen.

direction before accelerating away again. This behaviour develops with age from the
more harmonic oscillation—called pendular nystagmus—found in young children.

A SIMPLE MATHEMATICAL MODEL

We might suppose that congenital nystagmus is due to an instability of one of the
oculomotor control systems and attempt to build a model which has the possibility
of such an instability. For the purposes of this article we shall concentrate on an
instability mechanism which is based in the saccadic control system. The saccadic
system is the one which enables us to move our eyes rapidly and precisely. Saccades
are the jerk movements you are using now to scan the text as you read this page.
They are distinguished from the smooth pursuit eye movements (which you used to
follow the trajectory of that annoying fly) because during a saccade, visual perception
is turned off—there is no sense of a moving visual field as you move your eyes.

Saccades are caused by neurons in the brainstem (called bursters) which stimulate
the ocular muscles. The ocular muscles provide the physical control of our eyes.
A simple view of this would be to say that there are muscles which can rotate the
eye to the right and muscles which can rotate the eye to the left (actually the eye
can also rotate up and down and undergo torsional motion, so this is clearly an
over-simplification), and that there are bursters associated with these. Rather than
describe the individual behaviour of a large set of bursters, we shall try to characterise
the overall activity (for example, the mean firing rate) of populations of the different
classes of bursters. Here we shall consider just two classes which correspond to left
and right eye movements.

To begin with, let us denote the difference in the activity of the left and right
bursters as b. A basic model for the time evolution of this quantity can then be

written:

$$(1) \qquad \varepsilon \frac{db}{dt} = -b + f(\Delta g - s)$$

$$(2) \qquad \frac{ds}{dt} = b$$

The function $f : \mathbb{R} \to \mathbb{R}$ represents the response of the bursters to an error signal and is usually modelled as a sigmoidal function $f(x) = \text{sgn}(x)\alpha'(1 - e^{-|x|/\beta'})$ (here α' is the saturated response and β' sets the scale over which, say, the response is approximately linear). The quantity s is just the integrated burster activity and the quantity Δg indicates the required angular displacement of the eye. It is usually argued that s—which is a measure of how far the eye has moved and is used to provide feedback for the control system—is generated by a "resetable neural integrator". The epithet "resetable" refers to the fact that for this method to work s has to be set to zero at the beginning of each saccade.

The model is an example of a so-called "fast-slow" system; the quantity ε is usually taken to be small and represents the timescale on which the bursters respond to external stimulus. There is a standard way to analyse such systems. If we assume that the magnitude of the time derivative of b is of order unity then to lowest order in ε the left hand side of equation (1) can be ignored and the system reduces to a first order ordinary differential equation subject to an algebraic constraint

$$(3) \qquad b = f(\Delta g - s)$$

$$(4) \qquad \frac{ds}{dt} = b$$

When the constraint is not approximately satisfied this reduced-order model is invalid; the full second order system must be used. In this case we expect b to evolve rapidly since the magnitude of $\frac{db}{dt}$ must be at least of order ε^{-1}. Figure 2—which shows the result of numerical integration of equations (1) and (2)—illustrates how good a description this provides. The curve $b = f(\Delta g - s)$ is an attracting manifold (often referred to as the *slow manifold*). Trajectories which are not on this curve move rapidly—and approximately vertically—until they are close to the curve which they then follow. The comparatively slow motion near to the attracting manifold can be understood in terms of the sign of b: on the part of the curve for which $b > 0$—according to equation (4)—s is an increasing function of time; conversely s decreases when $b < 0$. It follows that the point at which the manifold crosses the s-axis (the point $(\Delta g, 0)$) is an attracting fixed point of the system.

To relate the activity of the burster neurons to actual eye movements we need to introduce some additional detail to the model. Measurements made of the physical characteristics of the eye as it moves in its socket under the influence of the muscles, indicate that is can be represented reasonably accurately as a second order linear system—basically a highly-damped, harmonic oscillator—driven by the burster activity. If we denote the rotation of the eye away from the forward direction as g and the eye velocity as v, this part of the model can be written as:

$$(5) \qquad \frac{dg}{dt} = v$$

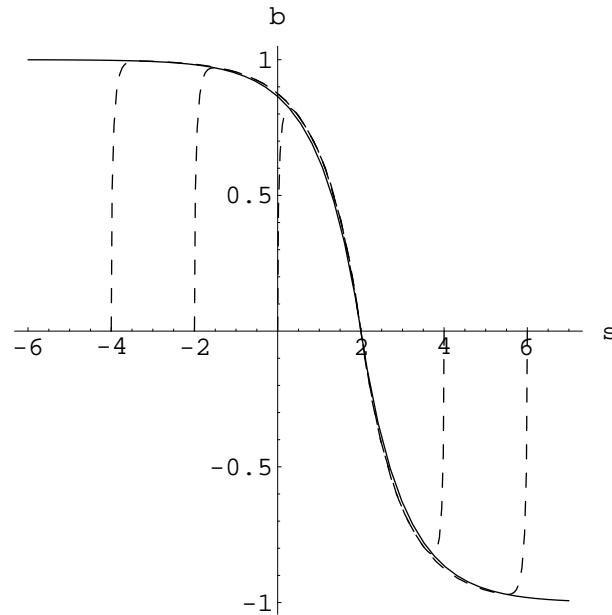$$(6) \qquad \frac{dv}{dt} = -(\frac{1}{T_1} + \frac{1}{T_2})v + \frac{-g + n + (T_1 + T_2)b}{T_1 T_2}$$

FIGURE 2. Numerically integrated trajectories (dashed lines) of the simple burster system given in equations (1) and (2), together with a plot (solid line) of $b = f(\Delta g - s)$. Here $\Delta g = 2$, $\alpha' = \beta' = 1$, $\varepsilon = 0.01$ and the initial conditions for the trajectories are given by $b(0) = 0$ and $s(0) = \{-4, -2, 0, 4, 6\}$.

where T_1 and T_2 are time constants of the linear system. As well as a term in b this system is driven by a quantity n which is, in effect, the integral of b.

$$(7) \qquad \frac{dn}{dt} = -\frac{n}{T_N} + b$$

This extra term provides persistence of the eye position following the saccade. (It is known that following a saccade the eye can remain fixed in its new position for long periods.) Equation (7) represents the behaviour of a so-called "neural integrator", T_N is the time constant of the neural integrator and is generally of the order of 25s in humans.

Taken together, these equations constitute a driving system (the burster system given by equations (1) and (2)) and a driven system (given by equations (5)–(7)). In the case of sufficiently small ε they provide a good qualitative description of normal saccades. Looking ahead to figure 4, plot 1 shows $g(t)$ for a normal saccade showing the rapid eye movement from $g = 0$ to $g = \Delta g(= 2)$ followed by long-term persistence of the eye in its new position. (Actually this plot was generated using the more sophisticated model introduced in the next section, but in this case the form of $g(t)$ is indistinguishable from that produced by the simple model.) The problem is, of course, that there is very little that can go wrong with this system; in particular, it offers no explanation of congenital nystagmus.

A BILATERAL MODEL

Equations (5) and (6) represent the behaviour of a well-understood, passive mechanical system. It is unlikely that the origins of congenital nystagmus are to be found
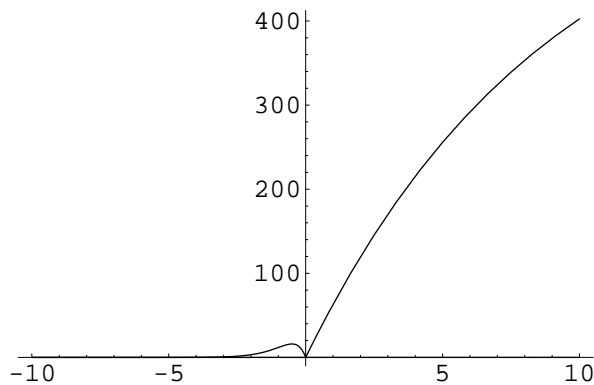
FIGURE 3. *A typical burster response plot, $F(x) = f(x) + h(x)$ as a function of the error x. This response shows an "on" response for positive errors. For larger positive values of x than are shown here $f(x)$—and hence $F(x)$—saturates to α'.*

here. There have been suggestions that an instability in the neural integrator could be responsible [4]. However, (while this may be true) the lack of any kind of detailed understanding of how a neural integrator is manifested physically means that any modification of equation (7) (to provide a mechanism for the instability) essentially degenerates into an exercise in the mathematical reverse-engineering of congenital nystagmus waveforms. On the other hand, quite a lot is known about the behaviour of bursters. In particular, we became interested in the work of Van Gisbergen *et al* [3] who studied the activity of burster cells in monkeys.

Van Gisbergen *et al* observed the activity of individual burster cells during a saccade and at the same time measured the corresponding eye movements. They were thus able to plot activity (meaning firing rate) of a single cell as a function of (essentially) the quantity we have called $\Delta g - s$. Their results from individual cells were reproducible, but they found that the form of the response varied from cell to cell. Nevertheless, a general pattern emerged from their experimental data. Most noticeably, bursters could be classified into two populations: those that were most active for positive $\Delta g - s$; and those most active when $\Delta g - s$ was negative. This observation corresponds to our earlier remark that there are (at least) two classes of burster corresponding to ocular muscles attached to the right and to the left sides of the eye. When $\Delta g > 0$, say, the eye needs to move to the right and so bursters which stimulate the contraction of the ocular muscles on the right of the eye are most active. Although the actual response was found to differ from cell to cell, the same basic form was found; in the case of the right bursters, for example, the activity increases monotonically from zero when $\Delta g - s = 0$ and saturates at large positive values of $\Delta g - s$. This response—which is sometimes called the "on" response—is essentially the sigmoid, f, introduced earlier, taken over the positive half of its domain.

Interestingly, Van Gisbergen *et al* also found that bursters have an "off" response, where, for example, right bursters are not entirely silent when $\Delta g - s < 0$, but have a small response at moderately negative values of $\Delta g - s$. This behaviour is sometimes referred to as the "braking response" because it causes a brief tug near to the end of a saccade by the muscles on the opposite side of the eye to those which caused the eye movement.

Combining the on and off responses, we can represent the response of a typical right burster as a non-negative, continuous, piecewise smooth function

$$(8) \qquad\qquad F(x) = f(x) + h(x)$$

where $f(x)$ and $h(-x)$ are smooth functions defined on the positive real line and such that $f(0) = h(0) = 0$. Both $f(x)$ and $h(-x)$ have a strictly positive gradient at the origin. However, $h(-x)$ has a small maximum before it decays rapidly and monotonically to zero as $x \to \infty$. For concreteness, we write:

$$(9) \qquad\qquad f(x) = \begin{cases} \alpha'(1 - e^{-x/\beta'}) & \text{if } x > 0 \\ 0 & \text{if } x \le 0 \end{cases}$$

and

$$(10) \qquad\qquad h(x) = \begin{cases} 0 & \text{if } x > 0 \\ -\alpha\frac{x}{\beta}e^{x/\beta} & \text{if } x \le 0 \end{cases}$$

We have now made explicit the suggestion that the on response, f, is just the restriction of the sigmoid function (also called f and defined earlier) to the positive half line. The new quantities α and β which parameterise the off response, h, correspond respectively to its maximum value (which is actually αe^{-1}) and the size of the error at which this maximum response occurs. A typical plot of F is shown in figure 3. Written in this way $F(x)$ represents the right bursters which give a large response when $x > 0$; we shall represent the behaviour of the left bursters by the function $F(-x)$. For suitable choices of the parameters α, β, α' and β' we can think of $F(x)$ and $F(-x)$ as giving the mean responses of the populations of right and left bursters.

Van Gisbergen *et al* made a further observation, which turns out to be crucial; that activity in either of the two populations of bursters tends to inhibit activity in the other. Unfortunately, it is difficult to quantify this effect. We really require a more sophisticated model of the connectivity of the populations of neurons. For the moment we shall be deliberately vague.

A model which has a similar structure to the simple model discussed above but which incorporates the experimental findings of Van Gisbergen *et al* is as follows:

$$(11) \qquad\qquad \varepsilon\frac{dr}{dt} = -r(1 + \gamma\Gamma(l)) + F(\Delta g - s)$$

$$(12) \qquad\qquad \varepsilon\frac{dl}{dt} = -l(1 + \gamma\Gamma(r)) + F(s - \Delta g)$$

$$(13) \qquad\qquad \frac{ds}{dt} = r - l$$

Now we are considering separately the activity of the populations of right (r) and left (l) bursters. Again, the parameter ε represents a timescale for the change in burster activities. Activity is generated as the response (given by F) to the error signal $\Delta g - s$ and tends to decay spontaneously. There is an extra contribution to this decay, $\gamma\Gamma$, which is due to inhibition. Here $\gamma \ge 0$ is a formal parameter which represents the strength of the inhibition and Γ—which represents the inhibitory effect of the activity of the other type of burster—is a positive, increasing function of its argument. Equation (13) is just the same as equation (2) with the relative activity written as $b = r - l$.
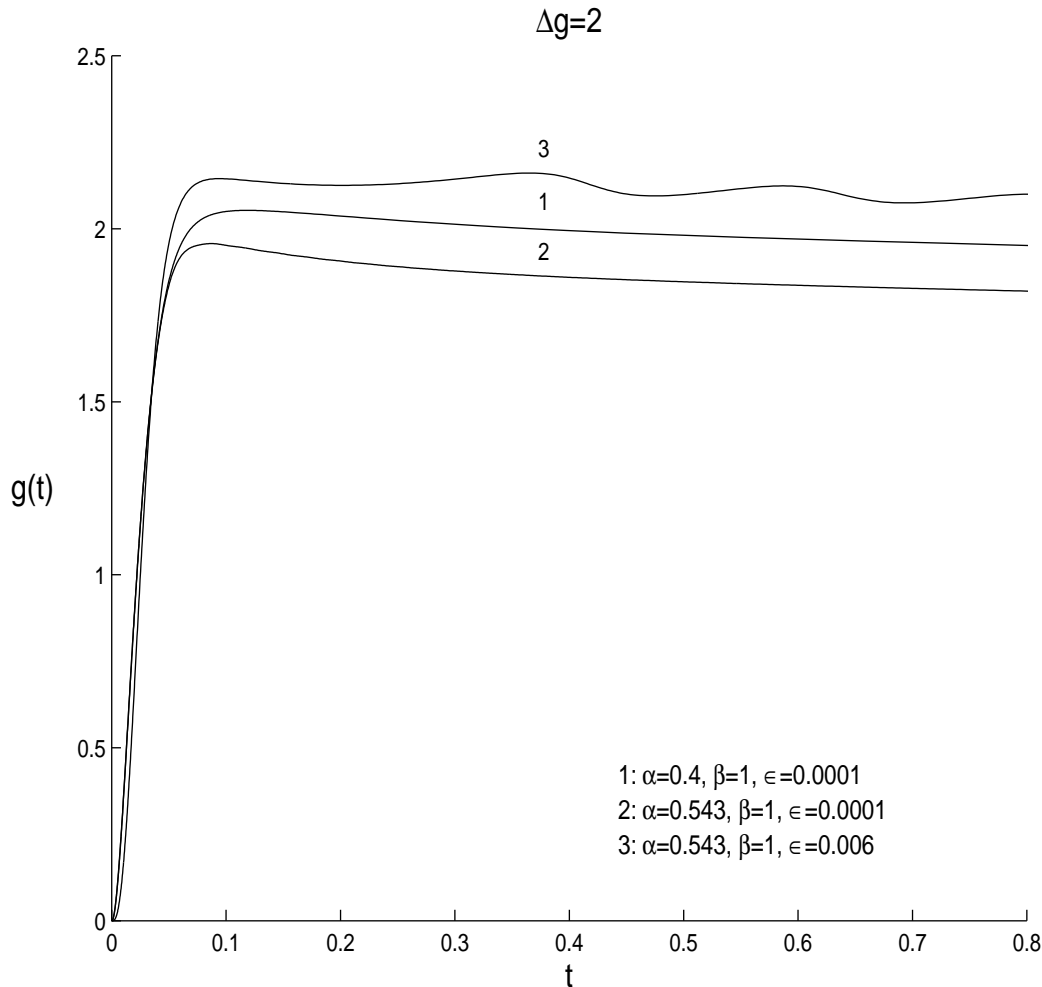
FIGURE 4. Plots showing the time dependence of eye position during a saccade obtained by numerical integration of the bilateral burster system given in equations (11)–(13) driving the plant equations (5)–(7). In each case the desired size of the saccade is given by $\Delta g = 2$. Plot 1 shows a normal saccade and is essentially the same as would be generated by the simple burster system; plot 2 shows an inaccurate saccade generated by an abnormal braking response; and plot 3 shows a small amplitude oscillation which can result for larger values of ε.

Figure 4 shows various saccades generated by numerical integration of equations (5)–(7) driven by our bilateral burster model. (For this numerical work we use $\Gamma(x) = x^2$—there is a discussion of this point below. Here and subsequently we fix $\alpha' = 600$ and $\beta' = 9$. These values are chosen on biological grounds.) In each plot the desired size of the saccade is given by $\Delta g = 2$. Plot 1 shows a normal saccade and is indistinguishable from saccades generated by the simple burster system—demonstrating that this model too is able to reproduce normal eye movements. However, in plot 2 we see that it is possible to obtain inaccurate saccades by increasing the magnitude of the off response of the bursters. Plot 3 shows that, if the response of the bursters is made more sluggish by increasing ε, we can generate a saccade which ends in a decaying oscillation. Before we go further with these observations, let us first try to

understand the nature of the changes we have introduced by going from the simple burster model to the bilateral model.

A Reduced Bilateral Model

If we subtract equation (12) from equation (11) and introduce $b = r - l$ and $B = r + l$ we get

$$(14) \qquad \varepsilon\frac{db}{dt} = -(b + \frac{1}{2}\gamma J(B,b)) + F(\Delta g - s) - F(s - \Delta g)$$

The term $J(B, b)$

$$(15) \qquad J(B, b) = (B + b)\Gamma((B - b)/2) - (B - b)\Gamma((B + b)/2)$$

which is a consequence of the inhibition between left and right bursters, is the only term in equation (14) to depend on B, the total burster activity. Thus, without inhibition ($\gamma = 0$) or, interestingly, in the case that there is inhibition but that the function Γ is linear, the bilateral model reduces to something like the simple model we introduced at the beginning.

$$(16) \qquad \varepsilon\frac{db}{dt} \;=\; -b + F(\Delta g - s) - F(s - \Delta g)$$

$$(17) \qquad \frac{ds}{dt} \;=\; b$$

Although there is an additional equation (obtained by adding equations (11) and (12)) which gives the time evolution of the total activity, in the case that either $\gamma = 0$ or Γ is linear, this is completely decoupled from the problem and, in particular, plays no role in determining eye movements. Indeed, if we ignore the contribution of the off response, h, to F we see that $F(\Delta g - s) - F(s - \Delta g)$ is exactly the sigmoidal function introduced in equation (1) so that in this case we have the come full circle by deriving the simple model as a special case of the bilateral model.

Even with the off response included, the reduced bilateral model has a rather restricted range of behaviour. Clearly equations (16) and (17) can be understood using the same arguments as were used with equations (1) and (2). In particular, we expect the behaviour to be dominated by the slow manifold

$$b = F(\Delta g - s) - F(s - \Delta g)$$

There are two situations which are distinguished by how quickly the braking response is applied. On the one hand—if the initial slope of h has magnitude less than that of f—we find a picture which looks like figure 2. If, however, the initial slope of h exceeds the initial slope of f, then the manifold crosses the s-axis three times as shown in figure 5. In both cases the dynamics on the slow manifold can be understood in terms of the sign of b. Obviously, in the first case, there is a single attracting fixed point at $(\Delta g, 0)$. In the second case, however, in addition to $(\Delta g, 0)$ there are two additional fixed points, one to either side. It is these fixed points which are attracting; the point $(\Delta g, 0)$, which corresponds to the accurate saccade, repels nearby points on the manifold. Thus we see that the difference between the slopes of f and h at the origin can be taken to be a bifurcation parameter. The bifurcation, which is marked by the creation of two new fixed points, has its counterpart in the unreduced bilateral system. The inaccurate saccade shown in plot 2 of figure 4 is due to the system being attracted to such a fixed point.
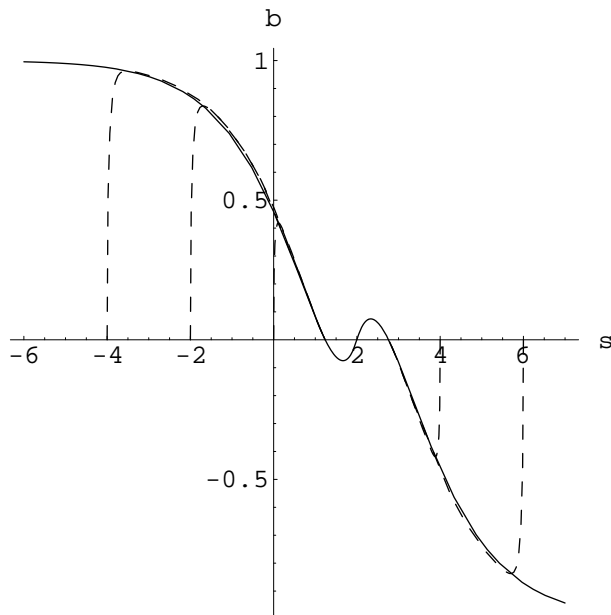
FIGURE 5. Numerically integrated trajectories (dashed lines) of the reduced bilateral burster system given by equations (14) (with $\gamma = 0$ or Γ a linear function) and (2), together with a plot (solid line) of $b = F(\Delta g - s)$. Here $\Delta g = 2$, $\alpha' = \beta' = 1$, $\alpha = 1.5$, $\beta = 1$, $\varepsilon = 0.01$ and the initial conditions for the trajectories are given by $b(0) = 0$ and $s(0) = \{-4, -2, 0, 4, 6\}$. In this case there are three fixed points corresponding to the three zero crossings of the graph of $F(\Delta g - s)$. Of these the central point—which corresponds to the accurate saccade—is unstable, while the fixed points to either side of this are stable.

THE BEHAVIOUR OF THE FULL BILATERAL MODEL

As we have already suggested, there is little information on which we can base a rational choice of the functional form of Γ. The results we report in this section are for the simplest nonlinearity we can choose: $\Gamma(x) = x^2$. The resulting model is quite rich in the different dynamical phenomena that it can exhibit. This section is, as a consequence, a broad overview which is rather short on detail.

Figure 6 gives a summary of the kind of behaviour that the bilateral model can exhibit as the parameters α and β are allowed to vary. (Recall that α and β correspond respectively to the maximum amplitude of the off response, and the magnitude of the error at which this response occurs.) The parameter space is shown divided into a number of regions which are labelled according to the attractors that exist at the corresponding values of the parameters. The regions marked **0** correspond to values of α and β such that the system has a unique fixed point at $(r, l, s) = (0, 0, \Delta g)$. (For brevity, we shall refer to the point $(0, 0, \Delta g)$ as **0**.) In these regions we expect to find normal—accurate—saccades. The labels $y_1^{\pm}$ correspond to symmetrically placed fixed points not **0**, and $\mathcal{C}_{\pm}$ correspond to a symmetric pair of limit cycles. (The fact that these non-trivial attractors appear in pairs is a simple consequence of symmetry. The vector field given by equations (11)–(13) commutes with the transformation $(r, l, s) \mapsto (l, r, 2\Delta g - s)$.) The curves which separate the various regions represent values of α and β where bifurcations occur.
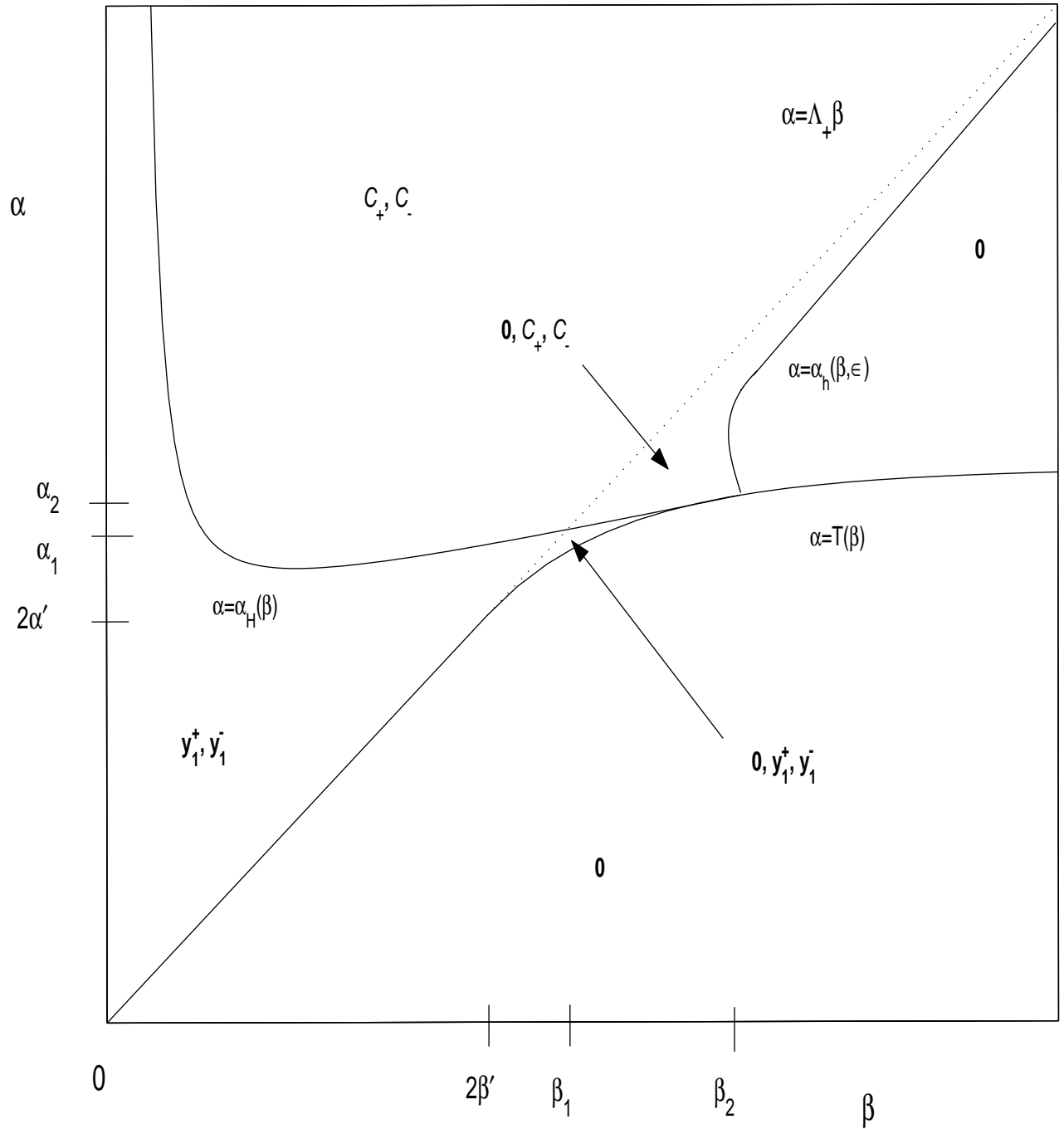
FIGURE 6. The bifurcations of the bilateral system as a function of α and β for suitably small values of ε. The diagonal line (marked $\alpha = \Lambda_+\beta$) indicates the "pitchfork" bifurcation which marks the creation of spurious fixed points caused by the braking response. The solid line represents a supercritical bifurcation and the dotted line a subcritical bifurcation. The curve $\alpha = T(\beta)$ shows a line of fold bifurcations which create a stable and unstable pair of spurious fixed points. The curve $\alpha = \alpha_H(\beta)$ shows a line of Hopf bifurcations which create a stable oscillation as a spurious fixed point loses stability. The curve $\alpha = \alpha_h(\beta)$ shows a line of homoclinic bifurcations at which the limit cycles are destroyed by colliding with an unstable fixed point created at the fold bifurcation.

The diagonal line represents the analogue in the full bilateral system of the bifurcation we observed in the reduced system. As we cross the solid part of this line by increasing α or decreasing β the system changes from having a single attracting fixed point at $\mathbf{0}$ (that is, the normal situation where there is a stable accurate saccade) to one having three fixed points; two "spurious" stable points (corresponding to inaccurate saccades) and the unstable point $\mathbf{0}$. The dotted line marks a subcritical version of the same bifurcation. As we cross the dotted line—going upwards and leftwards—two unstable spurious fixed points converge on $\mathbf{0}$. Beyond the bifurcation $\mathbf{0}$ is unstable. The point at which the diagonal line changes from solid to dotted is a bifurcation of higher codimension. The curved line marked $\alpha = T(\beta)$ which begins at this point is a line of fold bifurcations which marks the simultaneous creation of pairs of spurious fixed points (one stable and one unstable) not at $\mathbf{0}$.

The curve labelled $\alpha = \alpha_H(\beta)$ is a line of Hopf bifurcations on which each stable spurious fixed point loses stability to an attracting limit cycle oscillation. This curve meets the line of fold bifurcations at another bifurcation of higher codimension—this is found in a region where the vector fields are smooth and is known as a Takens-Bogdanov bifurcation point. It is known that a line of homoclinic bifurcations generically meets the fold and the Hopf lines at a Takens-Bogdanov point, and this is true here. The line marked $\alpha = \alpha_h(\beta, \varepsilon)$ is a set of parameters where the limit cycles are destroyed by colliding with an unstable fixed point created at the fold; that is, a line of homoclinic bifurcations.

The existence of limit cycle attractors of the unreduced bilateral model indicates that the model can account for oscillatory eye movements. For small ε—as in both the simple model and the reduced bilateral model described earlier—the bilateral model has a 1-dimensional, slow manifold which can constrain the observed global behaviour. The limit cycles generated by the Hopf bifurcation on the line $\alpha = \alpha_H(\beta)$ look like small ellipses for parameter values close to the bifurcation. However, as we move away from $\alpha = \alpha_H(\beta)$ the limit cycles grow steadily with change of parameter until they pass close to an attracting segment of the manifold. A subsequent small change in parameter can result in a limit cycle which is constrained to follow the attracting segment. Thus small changes in parameter can result in a huge change in the shape and amplitude of the limit cycle. This phenomenon known as a *canard*. The solid line in figure 7 shows an eye movement oscillation produced by a canard in the full bilateral model. The resemblance to the jerk nystagmus waveforms is rather striking. The slow flat part of the cycle corresponds to motion on the part of the slow manifold which is close to the fixed point at $\mathbf{0}$ (recall that this corresponds to an accurate saccade); the slow drift and fast return following this corresponds to the asymmetric shape of the slow manifold.

Figure 7 also shows two other kinds of oscillation that the model produces for larger values of ε than are represented in figure 6. The dashed line shows an oscillation produced by the glueing of the symmetric pair of limit cycles $\mathcal{C}_+$ and $\mathcal{C}_-$. At larger values of ε, the shape of this glued limit cycle loses all sense the structure imposed by the slow manifold. The dotted line in figure 7 shows a large amplitude, pendular oscillation which illustrates this point.
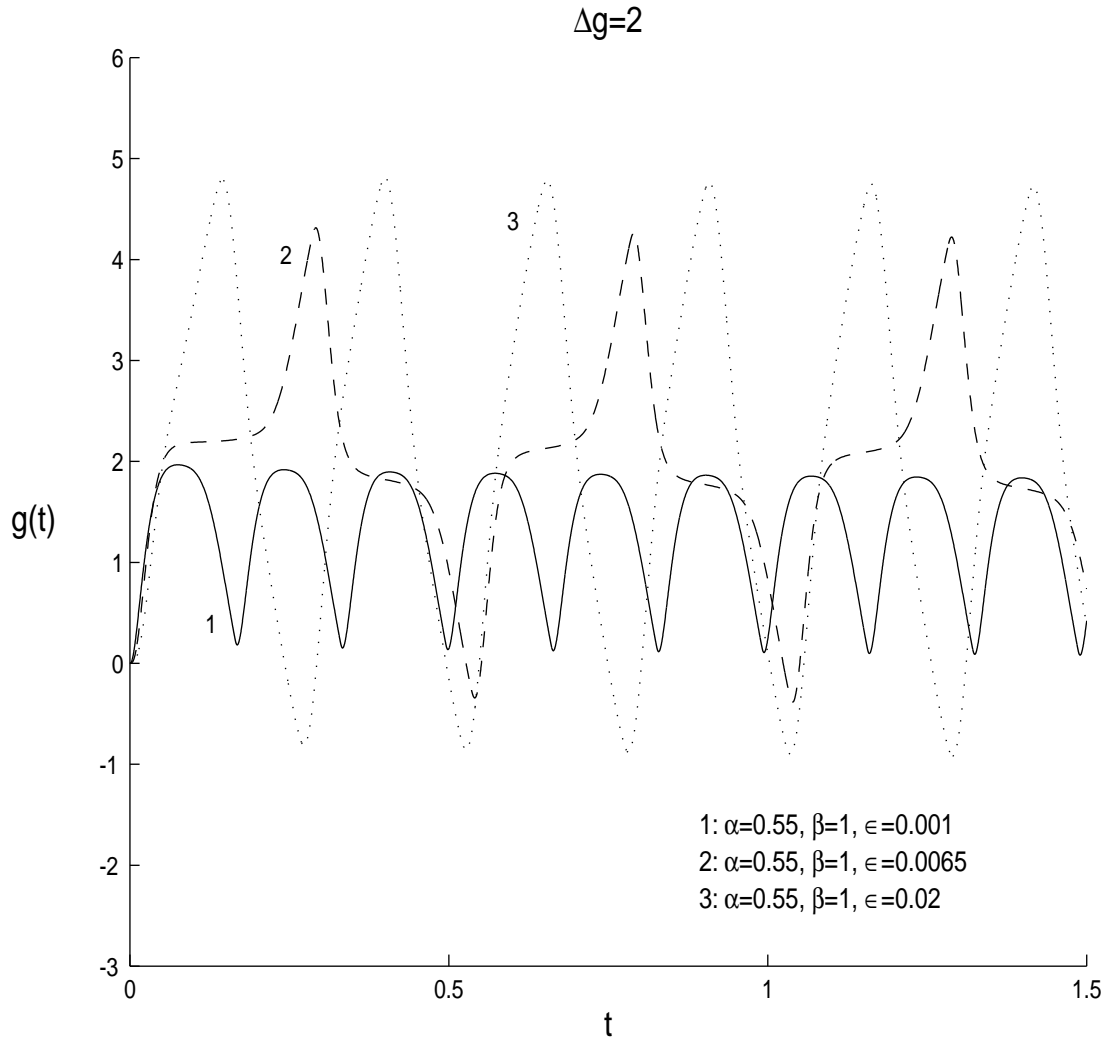
FIGURE 7. Plots showing the time dependence of eye position as in figure 4. The three curves show the effect of increasing ε. The solid curve shows a typical jerk nystagmus following a canard as the limit cycle interacts with the slow manifold. The dashed curve shows a two-sided oscillation following the glueing of two limit cycles related by the symmetry of the system. The dotted curve shows the kind of pendular oscillation that can result when motion on the slow manifold is no longer a good approximation.

SPECULATIONS AND SUMMARY

So we have learned something interesting. We have developed the basic model of saccadic control to obtain a bilateral burster model. However, we find that this model can be reduced to a simpler model (which is barely more complicated than the simple model we began with) unless there is inhibition between the two populations of bursters *and* the function Γ which models this is nonlinear. In the case of choosing Γ to be quadratic we find that the resulting model is rich enough to explain many different kinds of congenital nystagmus waveform. In particular, we find that jerk nystagmus

waveforms are a common consequence of a combination the burster braking response being too strong and burster-burster inhibition.

We are nearing the end of this article. Your ocular muscles have been working long and hard, but we hope that you are still game for one last burst(!) of activity. Are you willing to "go for the burn" [2] as we indulge in a little speculation?

Superficially, the kind of equations we have been considering resemble Law of Mass Action equations that arise in chemical kinetics or population dynamics. There is, however, an interesting distinction. The Law of Mass Action models the probability of collisions between reacting molecules dissolved in a fluid; if a reaction results from a collision between a molecule of species A and a molecule of species B, the rate of the reaction is proportional to the probability of collision which is modelled as the product of the concentrations of A and B. Since, generally, it is highly unlikely that three molecules will collide simultaneously it is unusual to find mass action kinetics which involve more than bilinear or quadratic terms. (When higher order terms are used in rate equations it is usually to represent the effect of a hidden, more complex, reaction mechanism.) In contrast, however, terms such as $-\gamma\Gamma(l)r$ which appears in equation (11) reflect the way that the burster cells are connected together. In particular, there is no reason to suppose (and much evidence to indicate the contrary) that neurons only connect pairwise. In this context then, mass action-like models should not be expected to be restricted to having bilinear and quadratic terms. We might interpret $\Gamma(l)$ as representing the number of active left bursters that are needed to suppress the activity of a right burster. Thus if Γ is linear we see something like a one-to-one relationship, a population of active left neurons are effective at suppressing a similar population of active right neurons. If, on the other hand, Γ is quadratic, we might suppose that it takes, on average, more like two active left bursters to suppress each active right burster. What is really needed is more statistical detail about how the bursters are connected. We might then hope to derive mass action type models as, perhaps, a limit giving the behaviour of large numbers of bursters. But this is another story.

References

[1] D. S. Broomhead, R. A. Clement, M. R. Muldoon, J. P. Whittle, C. Scallan, and R. V. Abadi. Modelling of congenital nystagmus waveforms produced by saccadic system abnormalities. *Biological Cybernetics*, 82:391–399, 2000.

[2] Jane Fonda, *Jane Fonda's Workout Book*, Allen Lane, Penguin Books, London. 1981

[3] J. A. M. Van Gisbergen, D. A. Robinson, and S. Gielen. A quantitative analysis of generation of saccadic eye movements by burst neurons. *J. Neurophysiology*, 45:417–442, 1981.

[4] L. M. Optican and D. S. Zee. A hypothetical explanation of congenital nystagmus. *Biological Cybernetics*, 50:119–134, 1984.

DEPARTMENT OF MATHEMATICS, UMIST, P.O. BOX 88, MANCHESTER M60 1QD, UNITED KINGDOM.
E-MAIL: OZGUR.AKMAN@STUD.UMIST.AC.UK

DEPARTMENT OF MATHEMATICS, UMIST, P.O. BOX 88, MANCHESTER M60 1QD, UNITED KINGDOM.
E-MAIL: D.S.BROOMHEAD@UMIST.AC.UK

THE VISUAL SCIENCES UNIT, THE INSTITUTE OF CHILD HEALTH, UNIVERSITY COLLEGE LONDON, 30 GUILFORD STREET, LONDON WC1N 1EH, UNITED KINGDOM.
E-MAIL: R.CLEMENT@ICH.UCL.AC.UK